Available online at www.sciencedirect.com

ScienceDirect

Procedia Engineering 130 (2015) 1677 – 1685

Procedia Engineering

www.elsevier.com/locate/procedia

14th International Conference on Pressure Vessel Technology

# Unified Correlation of In-Plane and Out-of-Plane Creep Constraints with Creep Crack Growth Rate

H.S. Ma[a], G.Z. Wang[a,*], F.Z. Xuan[a], S.-T. Tu[a]

[a]*Key Laboratory of Pressure Systems and Safety, Ministry of Education, East China University of Science and Technology, Shanghai 200237, China*

**Abstract**

In this paper, the equivalent creep strain distributions ahead of crack tips in different specimens were calculated by extensive finite element analyses, and the creep crack growth (CCG) rates of these specimens were simulated over a wide range of $C^*$. The capability and applicability of the constraint parameter $A_c$ for characterizing both in-plane and out-of-plane creep crack-tip constraints and establishing a unified correlation with CCG rate of a steel were investigated. Base on the parameter $A_c$, the unified correlation formulas of in-plane and out-of-plane constraints with CCG rate of a steel have been obtained.



Peer-review under responsibility of the organizing committee of ICPVT-14

*Keywords:* In-plane constraint; out-of-plane constraint; creep crack growth rate; equivalent creep strain; unified correlation; specimens

## 1. Introduction

Under creep conditions, a lot of experimental and theoretical evidences have shown that crack-tip constraint can affect creep crack growth (CCG) rate [1-8]. To accurately predict the creep life and achieve structural integrity assessments for high temperature components, it is important to quantify the creep crack-tip constraint levels. However, the studies for the creep constraint effects and the two-parameter or three-parameter characterization of creep crack-tip fields are very limited.

* Corresponding author. Tel.: +86-21-64252681; fax: +86-21-64253153.
*E-mail address:* gzwang@ecust.edu.cn



Peer-review under responsibility of the organizing committee of ICPVT-14
doi:10.1016/j.proeng.2015.12.337

In our previous work [9], by analogy to the unified constraint parameter $A_p$ based on the equivalent plastic strain for elastic-plastic fracture condition, a unified creep constraint parameter based on crack-tip equivalent creep strain was defined as follows [9]:

$$A_c = A_{CEEQ} / A_{ref} \quad \text{at } t/t_{red}=1 \tag{1}$$

Where $A_{CEEQ}$ is the area surrounded by the equivalent creep strain ($\varepsilon_c$) isoline ahead of a crack tip and $A_{ref}$ is the reference area surrounded by the $\varepsilon_c$ in a standard specimen, $t$ is creep time, and the $t_{red}$ is stress redistribution time. The $A_c$ represents a ratio of the $A_{CEEQ}$ of a specimen to the reference area $A_{ref}$ at the same $\varepsilon_c$ isoline, the same creep time $t/t_{red}$=1 and $C^*$ level. An increase in the parameter $A_c$ implies a loss of constraint.

In this work, the equivalent creep strain $\varepsilon_c$ distributions ahead of crack tips for specimens with different geometries and loading configurations (different in-plane and out-of-plane constraints) were calculated by FEM, and the CCG rates of these specimens are simulated over a wide range of $C^*$ by using stress dependent creep ductility and strain rate model in a ductility exhaustion based damage model. Based on the results, the capability and applicability of the parameter $A_c$ for characterizing both in-plane and out-of-plane creep crack-tip constraints and establishing a unified correlation with CCG rate for specimens with different geometries and loading configurations were investigated.

## 2. Finite element model and numerical procedures

### *2.1. Material*

The material used in this work is a Cr-Mo-V steel (Chinese 25Cr2NiMo1V steel). The true stress-strain curve of the steel at 566℃was shown in Fig. 1 [10].The Young's modulus $E$ and yield stress $\sigma_y$of the steel at 566℃ is 160GPa and 383MPa, respectively. For the Cr-Mo-V steel, the two-regime Norton (2RN) creep model in Eq. (2) has been developed in our previous work [10] by using the relation between minimum creep rate and stress, and the different Norton model parameters of ($A_1$, $n_1$) in low stress regime and ($A_2$, $n_2$) in high stress regime are listed in Table 1 [10]. This 2RN behavior of the Cr-Mo-V steel is similar to that of the 316H steel [11, 12].

$$\dot{\varepsilon} = \begin{cases} A_1\sigma^{n_1} & \sigma \le 250\,\mathrm{MPa} \\ A_2\sigma^{n_2} & \sigma > 250\,\mathrm{MPa} \end{cases} \quad \text{2RN model} \tag{2}$$

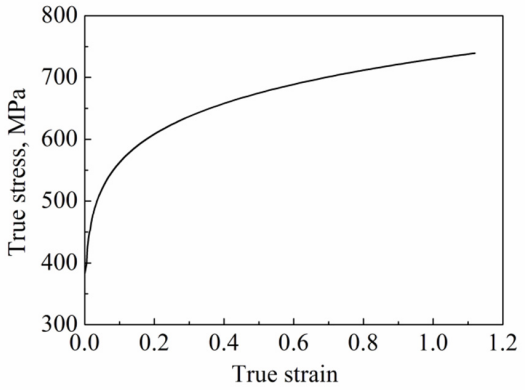


Fig. 1. The true stress-strain curve of the Cr-Mo-V steel at 566℃ [10].

Table1.The 2RN creep model parameters[10].

| Stress | $A$(MPa$^{-n}$h$^{-1}$) | $n$ |
|---|---|---|
| σ<250MPa | $A_1$=7.26×10$^{-26}$ | $n_1$=8.75 |
| σ≥250MPa | $A_2$=3.53×10$^{-36}$ | $n_2$=13.08 |

### *2.2. Specimens geometry and Finite element model*

Three sets of specimens with different loading configurations and geometries were used in FEM analyses. To investigate the in-plane constraint effect, four values of crack depths denoted as $a/W$= 0.2, 0.35, 0.5, and 0.7 were set for the two-dimensional (2D) plane strain SEN(B), SEN(T), and M(T) specimens. To investigate the out-of-plane constraint effect, four values of specimen thickness denoted as $B/W$= 0.1, 0.25, 0.5, and 1 were set for the three-dimensional (3D) specimens.

Due to symmetry in geometry, only half of the 2D plane strain M(T), SEN(B) and SEN(T) specimens and a quarter of the 3D M(T), SEN(B) and SEN(T) specimens were modeled. The typical finite element meshes for the 2D and 3D SEN(T) specimens ($W$ = 20 mm, $B$ = 10 mm and $a/W$ = 0.5) are illustrated in Figs. 2(a) and (b), respectively. The typical model in Fig. 2(a) contains 7751 four-node linear plane strain elements (CPE4H) and 7785 nodes, while it contains 63788 eight-node linear 3-D elements (C3D8H) and 72905 nodes in Fig. 2(b).The analyses have been carried out using ABAQUS code [13]. The local mesh distribution around the crack tip is shown in Fig. 2(c).

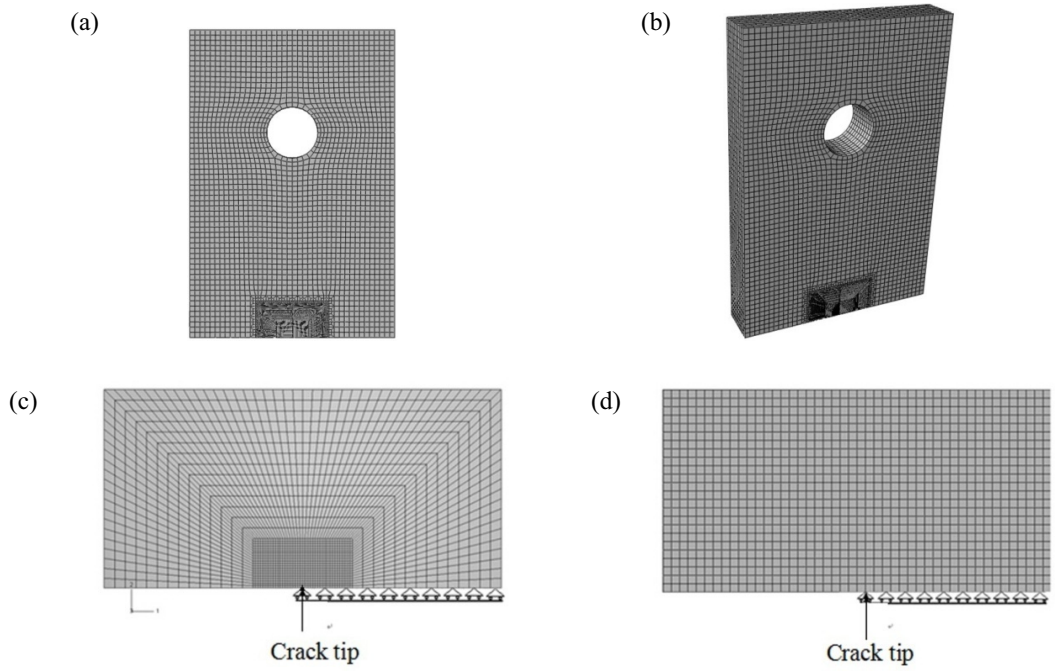


Fig. 2.Typical meshes in finite element models of 2D SEN(T) specimen (a), 3D SEN(T) specimen (b), typical local meshes around the crack region (c) and typical local meshes along the CCG region (d)

### *2.3. Creep damage model and creep crack growth simulation*

The creep crack growth rate of the specimens with different loading configurations and geometries (different in-plane and out-of-plane constraints) was simulated. The FEM models are the same as Figs. 2(a) and (b). The element

size in the crack growth zone is usually taken to be similar to grain size of the steels examined [14, 15]. For the Cr-Mo-V steel used in this study, the average grain size is estimated to be around 100μm [10, 16], thus the element size of 100μm is uniformly set in the crack growth zone, as shown in Fig. 2(d).

The ductility exhaustion based creep damage model has been widely used in the simulations of CCG rate [10, 14-16]. In this damage model, the rate of damage $\dot{\omega}$ is defined by the ratio of equivalent creep strain rate $\varepsilon_c$ and multiaxial creep ductility $\varepsilon_f^*$[10, 14-16].

$$\Delta\omega = \frac{\Delta\varepsilon}{\varepsilon^*_f} \tag{3}$$

And the total damage at any time is calculated from the time integral of creep damage accumulation rate in Eq. (4) [10, 14-16]:

$$\omega = \int_0^t \dot{\omega} dt = \int_0^t \frac{\dot{\varepsilon}_c}{\varepsilon^*_f} dt \tag{4}$$

where $\dot{\omega}$ is the creep damage rate, $\varepsilon_c$is the equivalent creep strain rate, and $\varepsilon_f^*$ is the multiaxial creep ductility. The value of damage parameter$\dot{\omega}$is between 0 and 1.

The Cocks and Ashby model [17] in Eq. (5) was widely used which is based on the cavity growth theory by power-law creep [10, 14-16]:

$$\frac{\varepsilon^*_f}{\varepsilon_f} = \sin\left[\frac{2}{3}\left(\frac{n-0.5}{n+0.5}\right)\right] / \sinh\left[2\left(\frac{n-0.5}{n+0.5}\right)\frac{\sigma_m}{\sigma_e}\right] \tag{5}$$

where the $\varepsilon_f^*$ and $\varepsilon_f$ are multiaxial and uniaxial creep ductility, respectively, and the $n$ is the creep exponent (for power law creep). The uniaxial creep ductility $\varepsilon_f$ in Eq. (5) is usually assumed to be a constant for a given temperature. However, a lot of experimental results and analyses have shown that the creep fracture mechanism depends on stress levels (strain rates), which leads to the stress-regime dependence of the creep ductility of materials [18-23]. The creep ductility can be expressed by Eq. (6) in a wide range of stress [10, 16].

$$\begin{cases} \varepsilon_{f1} & \sigma \le 225\text{MPa} \\ c_1\sigma^m + c_2 & 225 < \sigma \le 275\text{MPa} \\ \varepsilon_{f2} & 275\text{MPa} < \sigma \end{cases} \tag{6}$$

where $\varepsilon_{f1}$ and $\varepsilon_{f2}$ are lower shelf and upper shelf creep ductility, respectively, and $c_1$, $c_2$ and $m$ are constants ($c_1$=1.14×10$^{-14}$, $c_2$ =5.37×10$^{-3}$ and $m$=5.80). The lower shelf and upper shelf creep ductility were estimated to be $\varepsilon_{f1}$= 0.5 and$\varepsilon_{f2}$= 1.6, respectively. Eq. (6) was implemented in the ABAQUS code by a combination of user subroutine USDFLD and CREEP, and the CCG rates in a wide range of $C$* were simulated by using FEM for the specimens with different loading configurations and geometries .The true stress-strain curve of the steel in Fig. 1 and the 2RN creep model parameters in Table 1 were used.

## 3. Results and discussion

### *3.1. Creep crack growth rates in specimens with different in-plane and out-of-plane constraints*

To establish unified correlation of in-plane and out-of-plane creep constraints with CCG rates, the CCG rates in specimens with different in-plane and out-of-plane constraints need to be obtained for a wide range of $C$*. Figs. 3-5

(a) show the simulated *da/dt-C** curves for the 3D SEN(B), SEN(T) and M(T) specimens with different out-of-plane constraints (different *B*). Figs. 3-5 (b) show the simulated *da/dt-C** curves for the SEN(B), SEN(T) and M(T) specimens with different in-plane constraints (different *a*/*W*) in 2D plane strain (PE) . For a given specimen, a comparison between Figs. 3-5 show that the effect of out-of-plane constraint induced by specimen thickness *B* on CCG rate is more obvious than that of in-plane constraint induced by crack depth *a*/*W*. Thus, in CCG tests and life assessments, it should pay more attention on the effect of out-of-plane dimensions of specimens or components on CCG rate than that of in-plane dimensions, especially for the high constraint specimen or component geometries (such as SEN(B) and C(T) specimens).

### *3.2. Unified correlation of in-plane and out-of-plane creep constraints with creep crack growth rate*

It has been identified that the constraint parameters *T*, *Q*, $A_2$ and stress triaxiality factor *h* based on crack-tip stress fields are not a good unified representative of constraints, and a monotonic trend curve does not exist between these parameters and fracture toughness for various specimens with different in-plane and out-of-plane constraints under elastic-plastic fracture conditions [24-28, 29].It is necessary to identify whether or not the parameter $A_c$ can be used to establish the unified correlation of creep constraints with creep crack growth rates for the different specimen geometries with a wide of range in-plane and out-of-plane constraints.

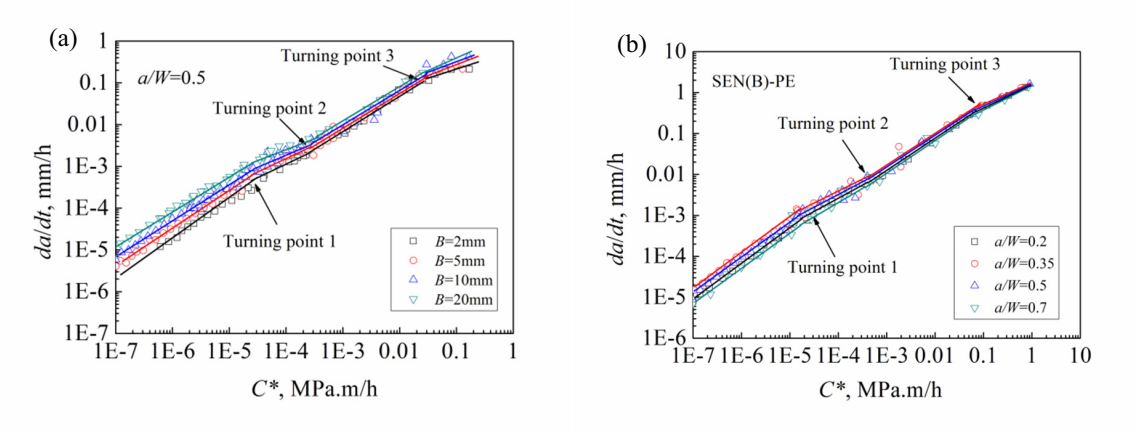


Fig. 3. Simulated CCG rate curves for the SEN(B) specimens (a) different out-of-plane constraints; (b) different in-plane constraints.

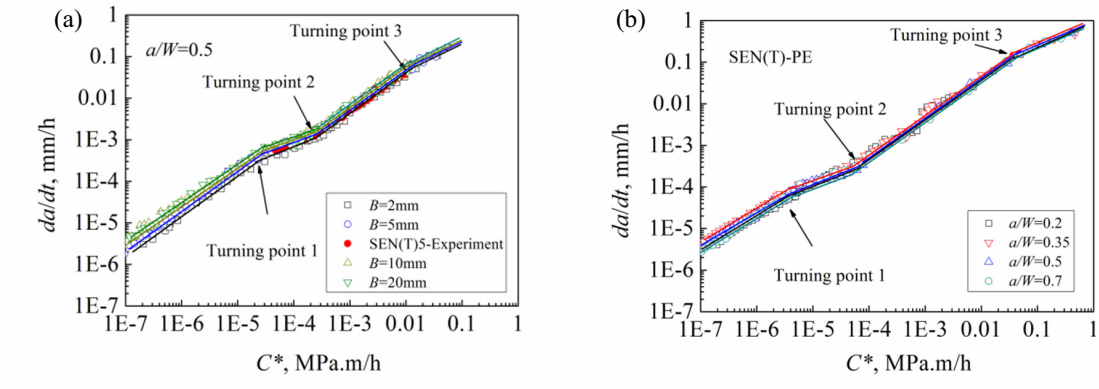


Fig. 4. Simulated CCG rate curves for the SEN(T) specimens (a) different out-of-plane constraints; (b) different in-plane constraints.

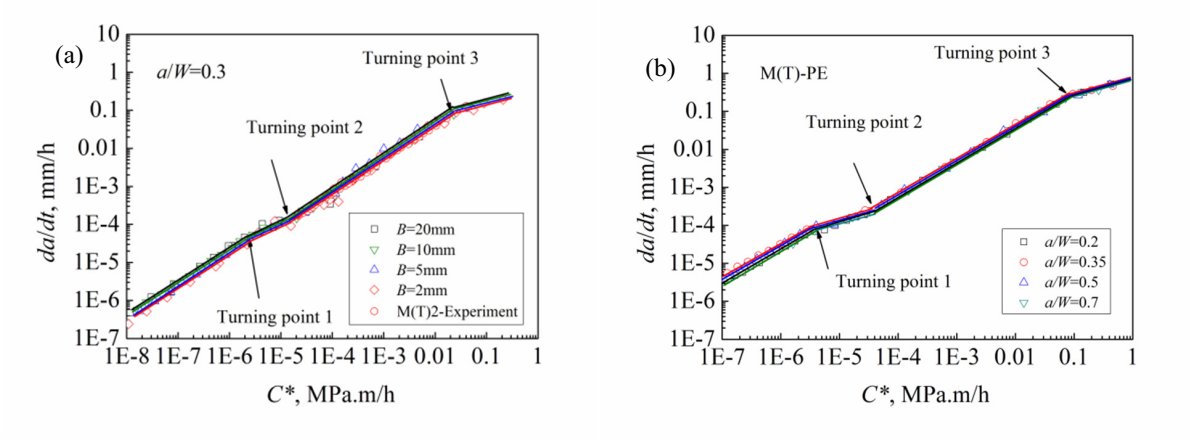


Fig. 5. Simulated CCG rate curves for the M(T) specimens (a) different out-of-plane constraints; (b) different in-plane constraints.

Based on the unified constraint parameter $A_c$, the relations between CCG rates and overall constraint levels in specimens or structures with different in-plane and out-of-plane constraints may be obtained. The CCG rates are usually expressed in the form [30],

$$\dot{a} = D_0 \, C^{*} \mathrm{q} \tag{7}$$

where $\dot{a}$ is CCG rate and in mm/h, $C^*$ is crack-tip fracture parameter and in MPa.m/h. The $D_0$ and $q$ are material constants which are often measured experimentally. When the constraint effect is considered, the CCG rate can be expressed as a function of $C^*$ and constraint parameter. The correlation lines calculated between CCG rates $da/dt$ and $A_c$ for two typical $C^*$ values at low $C^*$ region ($3\times10^{-7}$ MPa.m/h and $3\times10^{-6}$ MPa.m/h) and transition $C^*$ region ($3\times10^{-5}$ MPa.m/h and $3\times10^{-4}$ MPa.m/h) are shown in Figs. 6 (a) and (b), respectively. The data of the C(T) specimens in our previous work [9] are also included in Fig. 6.

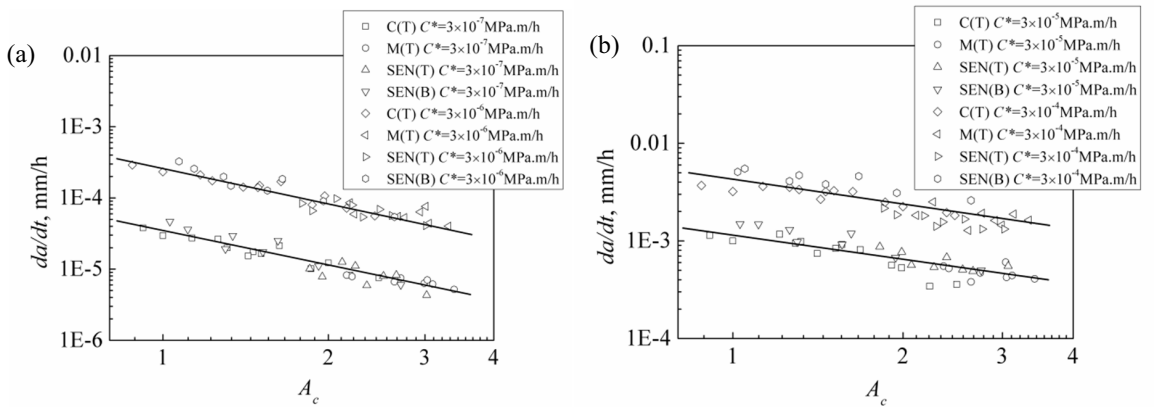


Fig. 6. The relations between CCG rates $da/dt$ and constraint parameter $A_c$for two typical $C^*$ values at low $C^*$ region ($3\times10^{-7}$MPa.m/h and $3\times10^{-6}$ MPa.m/h) (a) and transition$C^*$ region ($3\times10^{-5}$ MPa.m/h and $3\times10^{-4}$ MPa.m/h) (b) for all specimens with various in-plane and out-of-plane constraint levels (the standard specimen is the C(T) specimen with $W$ = 20mm and $a/W$ = 0.5 in plane strain)

The constraint dependent CCG rate $\dot{a}$ can be described in the following form [31],

$$\dot{a} = \dot{a}_0 \, f(A_c) \tag{8}$$

where $\dot{a}_0$ is the CCG rate from the standard specimen with high constraint, and $f(A_c)$ is a function of $A_c$. If the CCG rate in the high constraint C(T) specimen with $B$=10mm, $W$=2$B$=20mm and $a/W$=0.5 is taken to be the normalized CCG rate $\dot{a}_0$ and the CCG rate ratio $\dot{a}/\dot{a}_0$ is calculated for the four $C^*$ levels in Fig. 6, the relations between $\dot{a}/\dot{a}_0$ and the parameter $A_c$ can be established for the two $C^*$ regions, as shown in Fig. 7. It can be seen from Fig. 7 that there exists a linear relation on log-log scale between the $\dot{a}/\dot{a}_0$ and $A_c$ regardless of the specimens with different geometries, loading configurations, crack sizes and load levels $C^*$.

Power law relation can be used to fit the $\dot{a}/\dot{a}_0$- $A_c$ curves in Fig. 7. The fitting $\dot{a}/\dot{a}_0$- $A_c$ relations for the low $C^*$ region and transition $C^*$ region are shown in Eqs. (9) and (10).

$$f(A_c) = \dot{a}/\dot{a}_0 = 1.312 A_c^{-1.623}, \dot{a}_0 = 0.793 C^{*0.611} \tag{9}$$

$$f(A_c) = \dot{a}/\dot{a}_0 = 1.221 A_c^{-1.008}, \dot{a}_0 = 0.157 C^{*0.484} \tag{10}$$

The Eqs. (9) and (10) represent the relations between the CCG rates and the overall constraint levels composed of in-plane and out-of-plane constraints induced by different specimen geometries, loading configurations and crack sizes for a given material. These formulas may be used in constraint-dependent CCG life assessments of high-temperature structures with any in-plane and out-of-plane constraint levels.

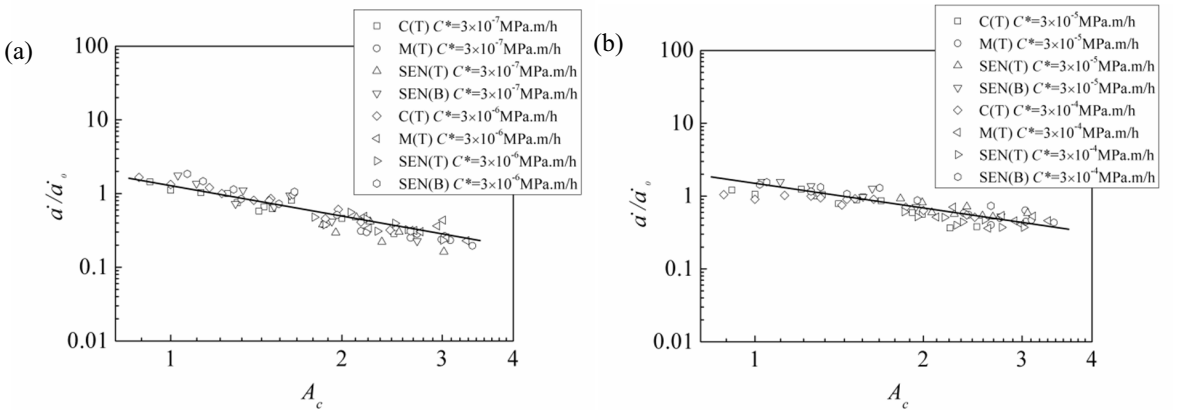


Fig. 7.The relations between $\dot{a}/\dot{a}_0$ and $A_c$for low $C^*$ region (a) and transition C* region (b) (the standard specimen is the C(T) specimen with $W$ = 20mm, $B$ = 10mm and $a/W$ = 0.5)

## 4. Conclusion

In this work, the equivalent creep strain $\varepsilon_c$ distributions ahead of crack tips for specimens with different geometries and loading configurations (different in-plane and out-of-plane constraints) were calculated by FEM, and the CCG rates of these specimens are simulated over a wide range of $C^*$ by using stress dependent creep ductility and strain rate model in a ductility exhaustion based damage model. The capability and applicability of the parameter $A_c$ for characterizing both in-plane and out-of-plane creep crack-tip constraints and establishing a unified correlation with CCG rate for specimens with different geometries and loading configurations were investigated. The main results obtained are as follows:

(1) In low(below turning point 1)and transition $C^*$ (between turning points 1 and 2) regions, the out-of-plane (induced by specimen thickness $B$) and in-plane (induced by crack depth $a/W$) constraints have effects on CCG rates, and with increasing the out-of-plane and in-plane constraints, the CCG rate increases. The effect of out-of-plane constraint on CCG rate is more obvious than that of in-plane constraint.
(2) The out-of-plane and in-plane constraint effects on the CCG rates are related to specimen geometries. The CCG rate of high constraint specimen geometry (such as SEN(B)) is more sensitive to the out-of-plane and in-plane constraints than that of low constraint specimen geometry (such as M(T)).
(3) The monotonic correlation lines between the CCG rate $da/dt$ and the constraint parameter $A_c$ on log-log scale can be formed for all specimens with different geometries, crack sizes and loading configurations. This further suggests that the parameter $A_c$ is a unified characterization parameter for a wide of specimen geometries and in-plane and out-of-plane creep constraints.

## Acknowledgments

This work was financially supported by the Projects of the National Natural Science Foundation of China (51375165, 51325504)

## References

[1] Bettinson A, O'Dowd N, Nikbin K, Webster G, Experimental investigation of constraint effects on creep crack growth, In: ASME 2002 Pressure Vessels and Piping Conference, Vancouver, BC, Canada, [PVP2002-1117], 2002.
[2] Tabuchi M, Kubo K, Yagi K, Effect of specimen size on creep crack growth rate using ultra-large CT specimens for 1Cr-Mo-V steel, Engng. Fract. Mech. 40 (1991) 311-321.
[3] Nikbin K, Justification for meso-scale modelling in quantifying constraint during creep crack growth, Mater. Sci. Eng. A. 365(2004) 107-113.
[4] Takahashi Y, Igari T, Kawashima F, Date S, Titoh N, Noguchi Y, Kobayashi K, Tabuchi M, High temperature crack growth behavior of high-chromium steels. In:18th International Conference on Structural Mechanics in Reactor Technology. Beijing, China, 2005, pp. 1904-1915.
[5] Budden P, Dean D, Constraint effects on creep crack growth. Eighth International Conference on Creep and Fatigue at Elevated Temperatures, San Antonio, Texas, USA: American Society of Mechanical Engineers, [CREEP 2007-26104], 2007.
[6] Tan JP, Tu ST, Wang GZ, Xuan FZ, Effect and mechanism of out-of-plane constraint on creep crack growth behavior of a Cr-Mo-V steel, Engng. Fract. Mech. 99 (2013) 324-334.
[7] Yokobori J, Yokobori T, Nishihara T, Yamaoka T, An alternative correlating parameter for creep crack growth rate and its application-Derivation of the parameter Q*, Mater. High. Temp. 10 (1992)108-18, Errata. 224.
[8] Yokobori J, Sugiura R, Tabuchi M, Fuji A, Adachi T, Yokobori T, The effect of multi-axial stress component on creep crack growth rate concerning structural brittleness. In: Proc of ICF11 in the content of high temperature and creep of CD Rom, 2005.
[9] Ma HS, Wang GZ, Xuan FZ, Tu ST, Unified characterization of in-plane and out-of-plane creep constraint based on crack-tip equivalent creep strain,Engng. Fract. Mech. 142 (2015) 1-20.
[10] Zhang JW, Wang GZ, Xuan FZ, Tu ST, Prediction of creep crack growth behavior in Cr-Mo-V steel specimens with different constraints for a wide range of C*, Engng. Fract. Mech. 132 (2014) 70-84.
[11] Mehmanparast A, Davies C, Webster G, Nikbin, Creep crack growth rate predictions in 316H steel using stress dependent creep ductility. Mater. High. Temp.31 (2014) 84-94.
[12] Mehmanparast A, Prediction of creep crack growth behaviour in 316H stainless steel for a range of specimen geometries, Int. J. Pres. Ves. Pip.120-121(2014) 55-65.
[13] Hibbitt, Karlsson, Sorensen, ABAQUS User's Manual, Version 6.10, 2011.
[14] Yatomi M, Nikbin K, O'Dowd N, Creep crack growth prediction using a damage based approach,Int. J. Pres. Ves. Pip. 80 (2003) 573-83.
[15] Oh C, Kim N, Kim Y, Davies C, Nikbin K, Dean D, Creep failure simulations of 316H at 550 C: Part I - a method and validation,Engng. Fract. Mech.78 (2011) 2966-77.
[16] Zhang JW, Wang GZ, Xuan FZ, Tu ST, In-plane and out-of-plane constraint effects on creep crack growth rate in Cr-Mo-V steel for a wide range of C*,Mater. High. Temp. DOI: http://dx.doi.org/10.1179/1878641314Y.0000000039,2014.
[17] Cocks A, Ashby M, Intergranular fracture during power-law creep under multiaxial stresses,Metal. Sci. 36 (1980) 237-49.
[18] Samuel E, Choudhary B, Palaparti D, Mathew M, Creep deformation and rupture behaviour of P92 steel at 923 K. Proc. Engng. 55 (2013) 64-9.
[19] Hales R, The role of cavity growth mechanisms in determining creep-rupture under multiaxial stresses,Fatigue. Fract. Engng. Mater .Struct.17 (1994) 579-91.

[20] Murakami E, Iwamoto T, Sawa T, New analytical approach to predict creep void growth in heat-affected zone of high Cr steel weldments. In:Proceedings of the ASME 2011 pressure vessels and piping division conference. Baltimore, Maryland, USA, 2011, [PVP2011-57510].
[21] Spinder M, The multiaxial creep ductility of austenitic stainless steels,Fatigue. Fract. Engng. Mater. Struct.27 (204) 273-81.
[22] Kim N, Kim Y, Davies C, Nikbin K, Dean D, Creep failures simulations for 316H at 550 0C. In: Proceedings of the ASME 2012 pressure vessels and piping division conference. Toronto, Ontario, Canada, 2012, [PVP2012-78133].
[23] Takahashi Y, Shibamoto H, Inoue K, Long-term creep rupture behavior of smoothed and notched bar specimens of low-carbon nitrogen-controlled 316stainless steel (316FR) and their evaluation,Nucl. Engng. Des.238 (2008) 310-21.
[24] Mostafavi M, Smith D., Pavier M, Fracture of aluminum alloy 2024 under biaxial and triaxial loading, Engng. Fract. Mech. 78 (2011) 1705-1716.
[25] Mostafavi M, Pavier M, Smith D, Unified measure of constraint. Manchester, UK, ESIA10, 2009.
[26] Mostafavi M, Smith D, Pavier M, Reduction of measured toughness due to out-of-plane constraint in ductilefracture of aluminium alloy specimens, Fatigue. Fract. Engng. Mater. Struct. 33 (2010) 724-739.
[27] Yang J, Wang G, Xuan F, Tu ST, Unified characterization of in-plane and out-of-plane constraint based on crack-tip equivalent plastic strain, Fatigue Fract. Engng. Mater. Struct. 36 (2012) 504-514.
[28] Yang J, Wang G, Xuan F, Tu ST, Unified correlation of in-plane and out-of-plane constraint with fracture toughness, Fatigue. Fract. Engng. Mater. Struct. 37 (2014) 132-145.
[29] Mu M, Wang G, Xuan F, Tu S, Unified parameter of in-plane and out-of-plane constraint effects and its correlation with brittle fracture toughness of steel, Int. J. Fract. 190 (2014) 87-98.
[30] Webster G, Ainsworth R, High temperature component life assessment. London: Chapman and Hall, 1994.
[31] Budden, P, Ainsworth, R, The effect of constraint on creep fractureassessments. Int. J. Fract. 97 (1999) 237-247.